American Journal of Modern Physics
2026, Vol. 15, No. 4, pp. 122–139
https://doi.org/10.11648/j.ajmp.20261504.12

Research Article

Magnetocaloric Effect and Magnetic Properties of Exciton Polaron in Monolayers Transition Metal Dichalcogenides Quantum Well

Edmond Ledoux Mbieda Posseu[1], Jean Valere Nguepnang[1, 2, *], Clautaire Mwebi Ekengoue[2, 3], Arthur Kitio Teguimfouet[1, 4], Gervi Mouketo Moussavou[5], Christian Kenfack-Sadem[1, 6], Lukong Cornelius Fai[1]

[1]Department of Physics, University of Dschang, Dschang, Cameroon

[2]Division of Scientific Research and Innovations, African Scientific Association for Innovative and Entrepreneurship (ASAIE), Dschang, Cameroon

[3]Faculty of Engineering and Technology, University of Buea, Buea, Cameroon

[4]Department of Physics, University of Yaounde I, Yaounde, Cameroon

[5]Department of Physics, University of Sciences and Technology of Masuku, Franceville, Gabon

[6]International Chair in Mathematical Physics and Applications (ICMPA-UNESCO Chair), University of Abomey-Calavi, Cotonou, Benin

Abstract

The magnetocaloric Effect (MCE) and magnetic properties of exciton-polaron in transition metal dichalcogenides quantum well was investigated. Using the Lee Low Pines method and an approximate diagonalization of exciton-phonon operators is achieved to investigate the ground and first excited states energies. Moreover, the partition function has been calculated using the grand canonical ensemble. Then, the entropy change well known as MCE, the magnetic susceptibility and the magnetization have been derived. Our results reveal that there is competition between thermal, magnetic field and quantum well contribution on the MCE, the magnetization and magnetic susceptibility. Dependent of the range of those parameters, this competition can exhibit interesting behavior such as high conventional magnetocaloric effect and local paramagnetism. We also found that magnetic field significantly affect the magnetic moment alignment and yield to statistical redistribution and reorganization of different states, moreover magnetic field drastically reduces disorder in the system. Likewise, results demonstrated that transition metal dichalcogenide materials offer several advantages such as magnetic stability, energetic robustness, gradual thermal control, predictable response, and a magnetocaloric effect exploitable over a wide temperature range due to its robustness and strong confinement. Tungsten disulfide (WS_2) material is more robust and sensitive whereas molybdenum diselenide ($MoSe_2$) material is more stable. The results obtained in this study can be used on sensitive thermomagnetic sensors, refrigerators and in data storage.

Keywords

Transition Metal Dichalcogenides, Quantum Well, Magnetic Properties, MCE, Exciton-polaron

*Correspondence: Jean Valere Nguepnang (bobovalere@yahoo.fr)

Received: 16 July 2026; **Accepted:** 28 July 2026; **Published:** 2 September 2026

1. Introduction

Condensed matter physics aims to establish a link between the macroscopic properties of solids and the microscopic interactions between a very large number of particles, particularly electrons and ions in the crystal lattice. The intrinsic complexity of these systems, described by a quantum many-body problem, generally makes any exact solution unattainable. In this context, the concept of quasiparticle emerges as a fundamental tool for describing the elementary excitations of interacting systems [1, 2]. It allows these excitations to be reformulated in terms of effective entities, analogous to independent particles but whose properties are renormalized by the surrounding medium [3]. Historically, the notion of quasiparticles was formalized within the framework of Fermi liquid theory developed by Landau to describe interacting electron systems [4, 5]. In this formalism, low-energy excitations near the Fermi surface can be interpreted as long-lived quasiparticles whose properties are modified by interactions with the rest of the system. This approach has successfully described the electronic properties of metals and now constitutes a central conceptual framework in the physics of many-body systems [5-7]. From a physical perspective, quasiparticles emerge as collective excitations resulting from the coupling between a local perturbation and the system's degrees of freedom. When an excitation is introduced, for example, by photon absorption, charge carrier injection, or the application of a magnetic field, the system's response is intrinsically collective [8]. The quasiparticle then corresponds to this composite entity, consisting of the bare particle and its cloud of excitations, providing an effective description of the system's dynamics [9].

Several fundamental quasiparticles play a central role in solid-state physics. Among the most emblematic examples is the phonon, which corresponds to the quantization of the collective vibrations of the crystal lattice [10]. Phonons are crucial in describing thermal conduction, electron-phonon interactions, and many transport phenomena in solids [11, 12]. Another important quasiparticle is the polaron, which arises from the strong coupling between a charge carrier and the vibrations of the crystal lattice. The displacement of this carrier induces a local deformation of the lattice, generating a polarization that feeds back on its dynamics. The resulting composite entity, formed by the charge carrier and the accompanying deformation cloud, constitutes a polaron whose effective properties, in particular mass and mobility, differ significantly from those of a free particle in the crystal [13].

In two-dimensional materials, such as semiconducting transition metal dichalcogenide monolayers, Coulombic interactions between an excited electron and the hole left in the valence band can lead to the formation of a quasi-neutral particle called an exciton. Excitons play a fundamental role in the optical properties of two-dimensional systems, particularly by dominating the absorption and emission of light near the electron gap [14]. In doped semiconductor systems, the presence of free carriers profoundly modifies excitonic physics by paving the way for the formation of more complex correlated states. In particular, the interaction between a photo-generated exciton and excess charge in the medium can lead to the formation of a trion, that is, a three-body bonded complex consisting of either two electrons and one hole, or two holes and one electron, depending on the nature of the doping [15-17]. However, trion formation is highly dependent on carrier density, temperature, and the dielectric environment. At low doping levels, the description in terms of bound trions generally remains appropriate, while at higher densities, the effects of many bodies, Pauli blockade, and coupling with the Fermi sea can profoundly alter the nature of optical excitations. In this regime, the boundary between the bound trion state and the dressed quasiparticle becomes subtler, and the optical response can evolve toward a description in terms of excitonic polarons rather than strictly defined trions [18, 19]. This transition illustrates the fact that optical excitations in doped semiconductors are not solely a matter of few-body physics, but also result from the interaction between excitonic complexes and the collective electronic environment [18, 19]. In transition metal dichalcogenide (TMD) monolayers, where excitonic effects are particularly pronounced, trions play a major role in optical dynamics, excitation relaxation, and valley-spin properties, making them central to understanding the optical response of doped systems [20].

Furthermore, these quasiparticles can also interact with each other to form other quasiparticles. This is the case, for example, in many two-dimensional materials where the interaction between excitons and phonons leads to the emergence of coupled states called exciton-polaron states, which play a central role in the dynamics of optical excitations and in the mechanisms of energy relaxation [20]. These states, arising from the interaction of excitons and phonons or an electron bath, lead to the formation of exciton-polarons.

In two-dimensional TMD monolayers, excitons dominate the optical response due to quantum confinement and the strengthening of Coulomb interactions [20, 21]. However, these excitations cannot be described independently of the crystal lattice, and their interaction with phonons leads to a substantial modification of their properties. This coupling is manifested, in particular, by a renormalization of exciton energies, a broadening of spectral lines, and the appearance of phonon replicas in absorption and photoluminescence spectra [22-24]. Thus, exciton-phonon coupling is a key element for understanding the optical and dynamic properties of two-dimensional materials [23-25]. At the microscopic level, exciton-phonon coupling results from the interaction between the electronic polarization associated with the electron-hole

bound state and the ionic shifts of the crystal lattice. The formation of an exciton induces a local perturbation of the electrostatic potential, which can generate a lattice response in the form of collective vibrations. In turn, these lattice fluctuations modify the energy landscape in which the exciton evolves, affecting its coherence, mobility, and relaxation mechanisms. The resulting quasiparticle is thus no longer a bare exciton, but a composite excitation whose effective properties incorporate the dynamic influence of the crystalline medium [26, 27]. A detailed understanding of this coupling is therefore essential for describing diffusion, thermalization, and decoherence processes in two-dimensional systems, and constitutes a major challenge for the development of optoelectronic and photonic devices based on the control of excitonic excitations [27].

TMD constitute a major class of layered materials that now occupy a central place in the physics of two-dimensional systems. Although these compounds have been known in bulk form for several decades, the isolation of atomically thin crystals has profoundly renewed their study by revealing qualitatively new electronic and optical properties. Following pioneering work on two-dimensional crystals exfoliated from laminated solids [28], TMD have emerged as an alternative to graphene due to the presence, in many of them, of an exploitable band gap. The demonstration of the direct nature of the band gap in the MoS_2 monolayer [29, 30] notably marked a turning point, showing that a layered material could become, at the atomic scale, a leading optically active semiconductor. This transition is accompanied by a significant strengthening of light-matter interactions and places TMD at the heart of research in optoelectronics and excitation physics in low-dimensional systems [31, 32]. From a structural and chemical perspective, TMDs are generally described by the formula MX_2, where M is a transition metal and X is a chalcogen (S, Se, or Te) [33]. Each layer consists of a metallic plane sandwiched between two chalcogen planes, forming a strongly bonded X-M-X unit within the plane, while interlayer interactions are dominated by van der Waals forces. This structure confers marked anisotropy to TMD and allows their exfoliation down to the monolayer. Several crystalline phases can be stabilized, notably the 2H phase with trigonal prismatic coordination, which is generally semiconducting, as well as the 1T and 1T′ phases, associated with metallic or semi-metallic behavior [34, 35]. This structural diversity, coupled with the rich chemical composition of possible combinations, offers a particularly wide range of engineering possibilities for modulating the electronic and optical properties of these materials. The physical properties of two-dimensional TMD exhibit remarkable characteristics, particularly in the monolayer regime. The transition from an indirect band gap in the bulk to a direct band gap in the monolayer is accompanied by a strong increase in photoluminescence and enhanced light-matter coupling [29, 30]. Furthermore, quantum confinement and weak dielectric screening lead to the formation of strongly bound excitons with high binding energies, making excitonic effects dominant even at room temperature [32]. In addition, strong spin-orbit coupling and valley physics due to the absence of an inversion center in some monolayers pave the way for phenomena such as spin-valley locking. These properties make TMD a prime platform for studying Coulomb interactions, correlation effects, and collective excitations in two-dimensional (2D) systems. TMD synthesis can be achieved using complementary approaches, ranging from top-down methods, such as mechanical or liquid exfoliation, to bottom-up approaches, including chemical vapor deposition (CVD), molecular beam epitaxy (MBE), and atomic layer deposition (ALD). The former allows for the production of very high-quality crystals suitable for fundamental studies, while the latter are essential for large-scale production and integration into devices. Controlling growth, crystalline phase, thickness, defects, and doping is a major challenge for optimizing the properties of magnetic flux-cored transistors (MFTs) and their technological exploitation. MFTs are attracting considerable interest due to their potential applications in numerous fields. Their band gap and atomic thickness make them promising candidates for next-generation field-effect transistors, while their strong light-matter interactions make them particularly well-suited for optoelectronic devices such as photodetectors, light-emitting diodes, and modulators [31, 36]. Their large specific surface area and chemical reactivity also open up possibilities in catalysis, sensors, and energy storage. Furthermore, their mechanical flexibility and sensitivity to stress allow for fine engineering of their properties through controlled deformation [37]. This unique combination of physical richness, structural versatility, and application potential explains the central role occupied today by TMD in research on 2D materials.

The application of a magnetic field is a fundamental tool for probing and controlling quasiparticles in condensed matter systems. In the presence of an external field, electronic and excitonic degeneracies are lifted, giving rise to Zeeman and diamagnetic energy shifts, as well as the quantization of energy levels into Landau levels in certain regimes. These effects provide access to intrinsic parameters of quasiparticles, such as the g-factor, effective radii, and renormalized binding energies. In two-dimensional systems, and particularly in TMD, the magnetic field also allows manipulation of spin and valley degrees of freedom, providing direct control over the fine structure of excitonic and correlated excitations [20, 38]. Confinement is another key parameter in quasiparticle physics, especially in low-dimensional systems. Dimensionality reduction and the modified dielectric environment lead to enhanced Coulomb interactions and decreased screening, favoring the formation of strongly correlated bound states. This confinement can be geometric, electrostatic, or dielectric in origin, and allows for increased spatial localization of quasiparticles, extended lifetimes, and modification of their dispersion. In two-dimensional materials, it plays a crucial role in stabilizing excitonic excitons, trions, and polarons, as well as in the emergence of new correlated phases absent in three-dimensional systems [39, 40]. The magnetic properties of quasiparticles

provide essential information about their internal structure and their coupling to the spin and valley degrees of freedom. They allow the exploration of spin-orbit coupling effects, degeneracy lifting, and interactions with a magnetic environment. In some systems, quasiparticles can also serve as probes of the material's magnetic order, offering an indirect way to characterize magnetic phases. These properties are particularly important for spintronic and valleytronic applications [41, 42].

The MCE which refers to the change in magnetic entropy of a system when an exterior magnetic field is applied to a magnetic material, is a remarkable property of a magnetic material. It was first discern by Emil Warburg in 1881 while grinding the application of magnetic field to iron materials. The use of an exterior magnetic field on magnetized materials generates a change in the magnetic state as well as on the structural rearrangement which may clue to the production of the variation in magnetic entropy [43]. It is necessary to note that the MCE is straight linked to the entropy change instigated by the exterior magnetic field. The MCE is one of the most mesmerizing and noteworthy portents in the field of quantum thermodynamics, engineering and materials sciences. It has gathered inordinate kindness due to wide range of applications, such as in magnetic refrigeration. This effect has sparked extensive research and exploration due to its promising potential in revolutionizing refrigeration technologies based on magnetic principles. Since the discover of the MCE many research have been done, both theoretically and experimentally **[**44-46**]**. Numerous remarkable works have been steered in this domain. For example, Alisultanov et al. [47] explored the MCE using a quasi-one-dimensional electron gas and derived analytical relationships for entropy changes. Rastegar et al. conducted a study on the magnetocaloric effect, magnetic susceptibility, and specific heat of tuned quantum dot/ring systems [48]. Their findings revealed that specific heat, magnetic susceptibility, and entropy change are all parameters that are influenced by variations in the magnetic field. They also observed that the entropy change exhibits a distinct minimum at low temperatures. Donfack et al. [49] investigated the magnetocaloric Effect (MCE) of a quantum pseudodot considering the influence of spin-orbit interaction, the entropy and internal energy change have been calculated using the Tsallis formulation. the results reveal that both the SOI effect and external parameters have a significant impact on the entropy and internal energy changes of a quantum pseudodot. It is important to note that the MCE is closely linked to the behavior of the magnetic dipoles, and the presence of external magnetic fields and SOI exert considerable influence on the entropy change. Nguepnang et al. [50] also studied the magnetocaloric effect (MCE) and the thermodynamic properties of the magnetopolaron in TMD using the canonical ensemble approach. They found that increasing the magnetic field significantly affects the alignment of the magnetic moment or provides additional energy in the monolayers of 2D TMD. In connection with the observed energy exchange, they also demonstrated how conventional TMD can have practical applications in magnetic refrigeration.

To date, several studies have been conducted on TMD, for example: Kenfack-Sadem and al. [51] studied the dynamics and decoherence of exciton-polaron in common transition metal dichalcogenides under the influence of a magnetic field barrier. They found that the motion of the excitonic polaron is accelerated by increasing the length of the magnetic barrier; Its transition from the valence band to the conduction band and its decoherence can be modulated by the magnetic field barrier. On the other hand, Temguimfouet and al. [52] studied the influence of a magnetic barrier and temperature on the optical and dynamic properties of the exciton-polaron in TMD. They found, among other things, that the magnetic barrier stabilizes the exciton-polaron system subjected to thermal perturbations. The entropy of the system is highly sensitive to the type of TMD monolayer, the length scale of the barrier, and the temperature. They also showed that the greater the magnetic length, the greater the disorder in the exciton-polaron system, and that the mobility and lifetime of the exciton-polaron decrease with increasing magnetic length. However, the magnetic properties of exciton-polarons in TMD remain largely unexplored. So, the current research work aims to study both MCE and magnetic properties of exciton-polaron embedded in 2D TMD quantum well through canonical ensemble approach. The rest of the article is organized as follows. In section 2, we describe the Hamiltonian of the system and use the diagonalization technique to determine its energy, then the canonical ensemble approach to derive its magnetic properties using the partition function. In section 3, the results and their discussion are presented, and we conclude in section 4.

2. Theoretical Model and Calculations

Let suppose an exciton-polaron in movement in a semiconducting TMD quantum well monolayer. The total Hamiltonian describing such system can be written as in Equation (1) below:

$$H = H_{ex,\rho} + H_{ph} + H_{ex-ph} + H_{ex,z} \tag{1}$$

To the right hand side of Equation (1), the Hamiltonian of the exciton in the x, y plane is represented by the first term, given by Equation (2) where E_g stands for the bandgap of the monolayer along the x, y direction, M is the mass of exciton, $\hbar$ is the reduced Planck constant, E_b the binding energy of exciton owing to the coulomb action that takes place between the electron and the hole in the surface plane of the monolayer and $C_k^{\dagger}, C_k$ are respectively creation and annihilation operators of exciton with the wave vector k. The Hamiltonian of the Phonon is presented by the second term and described by Equation (3), in which $b_q^{\dagger}, b_q$ are respectively

creation and annihilation operators of phonon with the wave vector q and energy ω. The third term is the aid of the electron and hole in the z-direction set by Equation (4), with $P_{i,z}, m_i$ respectively the momentum and mass of electron (i=e) and hole (i=h) and $U(z)$ the quantum well potential expressed by Equation (7). The last term is the Hamiltonian of the exciton-phonon interaction set by Equation (5), with $E^{op}(q)$ the exciton-phonon coupling function given by Equation (6) with S the normalization area, ρ the area mass density and u the sound velocity of the phonon mode, D_c and D_v denote respectively, the deformation potential constant for electron phonon interaction at the critical points (K, K') in the conduction band and the corresponding expression for hole in the valence band.

$$H_{ex,\rho} = \sum_k E_k^{ex} C_k^{\dagger} C_k = \sum_k \left(\frac{\hbar^2 k^2}{2M} + E_g - E_b \right) C_k^{\dagger} C_k \tag{2}$$

$$H_{ph} = \sum_q \hbar \omega_q b_q^{\dagger} b_q \tag{3}$$

$$H_z = \sum_{i=e;h} \left(\frac{P_{i,z}}{2m_i^*} + U_i(z_i) \right) \tag{4}$$

$$H_{ex-ph} = \sum_{k,q} E^{OP}(q) C_{q+k}^{\dagger} C_k \left(b_q + b_{-q}^{\dagger} \right) \tag{5}$$

$$E^{op}(q) = (D_c - D_v) \sqrt{\frac{\hbar q}{2S\rho u}} \tag{6}$$

$$U_i(z_i) = \begin{cases} 0 if z_i \le L \\ \infty else \end{cases} \tag{7}$$

With the help of the Lee-Low-Pines operator [29, 30] given by Equation (8), and using the Baker-Campbell-Hausdorff formula as indicated by authors of [30], the Hamiltonian of Equation (1) can be diagonalized and given by Equation (9).

$$U = e^{i \sum_{k,q} C_{k+q}^{\dagger} C_k \left[f_{ex}^*(k,q) b_{-q}^{\dagger} + f_{ex}(k,q) b_q \right]} \tag{8}$$

$$H = H_{ex,\rho} + H_{ph} + H_{ex,z} + H_{ex-ph}^{T2D} \tag{9}$$

With

$$H_{ex-ph}^{T2D} = \sum_{k,k',q} \left| E^{OP}(q) \right|^2 \left[\frac{1}{E_{k+q}^{ex} - E_k^{ex} - \hbar\omega} - \frac{1}{E_{k+q}^{ex} - E_k^{ex} + \hbar\omega} \right] C_q^{\dagger} C_{q+k} C_{q+k'}^{\dagger} C_{k'} \tag{10}$$

In order to obtain the states energies, we follow the authors of ref [15], Then using the waves functions given by Equation (11), where $n = 0$ stand for the fundamental state, $n = 1$ for the first excited state and ψ_k given by Equation (12), we obtained the fundamental and first excited states energies given Equation (13) and Equation (14).

$$\varphi_n = \psi_k C_k^{\dagger} |n\rangle |n_{ph}\rangle |n_e, n_h\rangle \tag{11}$$

$$\psi_k = \sin\left(\frac{\pi k z_e}{L} \right) \sin\left(\frac{\pi k z_h}{L} \right) \tag{12}$$

$$E_0 = \xi^2 + E_g - E_b + \frac{\hbar^2 k^2}{2M}(1 - B_{ex2}) - B_{ex1} + \frac{\pi^2 \hbar^2}{2\mu L^2} \tag{13}$$

$$E_1 = 4\xi^2 + 4E_g - 4E_b + 4\frac{\hbar^2 k^2}{2M}(1 - 2B_{ex2}) - 8B_{ex1} + \frac{2\pi^2 \hbar^2}{\mu L^2} \tag{14}$$

where μ is the reduced mass of the exciton defined by

$$\mu = \frac{m_e \times m_h}{m_e + m_h}$$

$$\xi^2 = \frac{3a_{ex}^2}{8} \left(\frac{1}{2M} + \frac{1}{2\mu} \right) B^2 \tag{15}$$

$$\begin{cases} B_{ex1} = \dfrac{\pi \sqrt{\hbar\omega} (D_c - D_v)^2}{\sqrt{2}\hbar^2 \rho u} (m_e + m_h)^{\frac{3}{2}} \\ B_{ex2} = \dfrac{3\pi (D_c - D_v)^2 (m_e + m_h)^{\frac{3}{2}}}{4\rho\mu\sqrt{\hbar\omega}\sqrt{2}} \left(\dfrac{\hbar^2 k^2}{2M} \right) \end{cases} \tag{16}$$

From these results and following the Tsallis formalism, the partition function can be derived as in Equation (17).

$$Z_\alpha = \sum_{j=0}^{1}\left[1-\beta(1-\alpha)E_j\right]^{\frac{1}{1-\alpha}} \tag{17}$$

Thus the magnetic properties such as magnetization and magnetic susceptibility are calculated and given respectively by Equation (18) and Equation (19).

$$M_\alpha = -\frac{\partial F_\alpha}{\partial B}$$

$$= -\frac{\frac{3a_{ex}^2}{8}\left(\frac{1}{M}+\frac{1}{\mu}\right)B\left[\begin{array}{l}\left(1-\frac{(1-\alpha)\left(\frac{3a_{ex}^2}{16}\left(\frac{1}{M}+\frac{1}{\mu}\right)B^2+E_g-E_b+\frac{\hbar^2k^2}{2M}(1-B_{ex2})-B_{ex1}+\frac{\pi^2\hbar^2}{2\mu L^2}\right)}{k_BT}\right)^{\frac{\alpha}{1-\alpha}} \\ +4\left(1-\frac{(1-\alpha)\left(\frac{3a_{ex}^2}{4}\left(\frac{1}{M}+\frac{1}{\mu}\right)B^2+4E_g-4E_b+4\frac{\hbar^2k^2}{2M}(1-2B_{ex2})-8B_{ex1}+\frac{2\pi^2\hbar^2}{\mu L^2}\right)}{k_BT}\right)^{\frac{\alpha}{1-\alpha}}\end{array}\right]}{\left[\begin{array}{l}\left(1-\frac{(1-\alpha)\left(\frac{3a_{ex}^2}{16}\left(\frac{1}{M}+\frac{1}{\mu}\right)B^2+E_g-E_b+\frac{\hbar^2k^2}{2M}(1-B_{ex2})-B_{ex1}+\frac{\pi^2\hbar^2}{2\mu L^2}\right)}{k_BT}\right)^{\frac{1}{1-\alpha}} \\ +\left(1-\frac{(1-\alpha)\left(\frac{3a_{ex}^2}{4}\left(\frac{1}{M}+\frac{1}{\mu}\right)B^2+4E_g-4E_b+4\frac{\hbar^2k^2}{2M}(1-2B_{ex2})-8B_{ex1}+\frac{2\pi^2\hbar^2}{\mu L^2}\right)}{k_BT}\right)^{\frac{1}{1-\alpha}}\end{array}\right]} \tag{18}$$

$$\chi_\alpha = -\frac{\partial^2 F_\alpha}{\partial B^2}$$

$$= \frac{1}{\left[\begin{array}{l}\left(1-\frac{(1-\alpha)\left(\frac{3a_{ex}^2}{16}\left(\frac{1}{M}+\frac{1}{\mu}\right)B^2+E_g-E_b+\frac{\hbar^2k^2}{2M}(1-B_{ex2})-B_{ex1}+\frac{\pi^2\hbar^2}{2\mu L^2}\right)}{k_BT}\right)^{\frac{1}{1-\alpha}} \\ +\left(1-\frac{(1-\alpha)\left(\frac{3a_{ex}^2}{4}\left(\frac{1}{M}+\frac{1}{\mu}\right)B^2+4E_g-4E_b+4\frac{\hbar^2k^2}{2M}(1-2B_{ex2})-8B_{ex1}+\frac{2\pi^2\hbar^2}{\mu L^2}\right)}{k_BT}\right)^{\frac{1}{1-\alpha}}\end{array}\right]} \times$$

$$\left[\frac{\left(\frac{3a_{ex}^2}{8}\left(\frac{1}{M}+\frac{1}{\mu}\right)\right)^2\alpha B^2}{k_BT}\left[\left(1-\frac{(1-\alpha)\left(\frac{3a_{ex}^2}{16}\left(\frac{1}{M}+\frac{1}{\mu}\right)B^2+E_g-E_b+\frac{\hbar^2k^2}{2M}\left(1-B_{ex2}\right)-B_{ex1}+\frac{\pi^2\hbar^2}{2\mu L^2}\right)}{k_BT}\right)^{\frac{2\alpha-1}{1-\alpha}}\right.\right.$$
$$\left.+16\left(1-\frac{(1-\alpha)\left(\frac{3a_{ex}^2}{4}\left(\frac{1}{M}+\frac{1}{\mu}\right)B^2+4E_g-4E_b+4\frac{\hbar^2k^2}{2M}\left(1-2B_{ex2}\right)-8B_{ex1}+\frac{2\pi^2\hbar^2}{\mu L^2}\right)}{k_BT}\right)^{\frac{2\alpha-1}{1-\alpha}}\right]$$
$$-\frac{3a_{ex}^2}{8}\left(\frac{1}{M}+\frac{1}{\mu}\right)\left[\left(1-\frac{(1-\alpha)\left(\frac{3a_{ex}^2}{16}\left(\frac{1}{M}+\frac{1}{\mu}\right)B^2+E_g-E_b+\frac{\hbar^2k^2}{2M}\left(1-B_{ex2}\right)-B_{ex1}+\frac{\pi^2\hbar^2}{2\mu L^2}\right)}{k_BT}\right)^{\frac{\alpha}{1-\alpha}}\right.$$
$$\left.+4\left(1-\frac{(1-\alpha)\left(\frac{3a_{ex}^2}{4}\left(\frac{1}{M}+\frac{1}{\mu}\right)B^2+4E_g-4E_b+4\frac{\hbar^2k^2}{2M}\left(1-2B_{ex2}\right)-8B_{ex1}+\frac{2\pi^2\hbar^2}{\mu L^2}\right)}{k_BT}\right)^{\frac{\alpha}{1-\alpha}}\right]$$
$$-\frac{\left(\frac{3a_{ex}^2}{8}\left(\frac{1}{M}+\frac{1}{\mu}\right)\right)^2B^2}{k_BT\times\left[\left(1-\frac{(1-\alpha)\left(\frac{3a_{ex}^2}{16}\left(\frac{1}{M}+\frac{1}{\mu}\right)B^2+E_g-E_b+\frac{\hbar^2k^2}{2M}\left(1-B_{ex2}\right)-B_{ex1}+\frac{\pi^2\hbar^2}{2\mu L^2}\right)}{k_BT}\right)^{\frac{1}{1-\alpha}}\right.}\times$$
$$\left.+\left(1-\frac{(1-\alpha)\left(\frac{3a_{ex}^2}{4}\left(\frac{1}{M}+\frac{1}{\mu}\right)B^2+4E_g-4E_b+4\frac{\hbar^2k^2}{2M}\left(1-2B_{ex2}\right)-8B_{ex1}+\frac{2\pi^2\hbar^2}{\mu L^2}\right)}{k_BT}\right)^{\frac{1}{1-\alpha}}\right]$$
$$\left[\left(1-\frac{(1-\alpha)\left(\frac{3a_{ex}^2}{16}\left(\frac{1}{M}+\frac{1}{\mu}\right)B^2+E_g-E_b+\frac{\hbar^2k^2}{2M}\left(1-B_{ex2}\right)-B_{ex1}+\frac{\pi^2\hbar^2}{2\mu L^2}\right)}{k_BT}\right)^{\frac{\alpha}{1-\alpha}}\right.$$
$$\left.+4\left(1-\frac{(1-\alpha)\left(\frac{3a_{ex}^2}{4}\left(\frac{1}{M}+\frac{1}{\mu}\right)B^2+4E_g-4E_b+4\frac{\hbar^2k^2}{2M}\left(1-2B_{ex2}\right)-8B_{ex1}+\frac{2\pi^2\hbar^2}{\mu L^2}\right)}{k_BT}\right)^{\frac{\alpha}{1-\alpha}}\right]^2 \quad (19)$$

$$\Delta S_\alpha = S_\alpha(T, B \neq 0, L) - S_\alpha(T, B = 0, L)$$

$$= \frac{1}{\alpha - 1}\left[\begin{array}{l}\left[\left(1 - \frac{(1-\alpha)\left(\frac{3a_{ex}^2}{16}\left(\frac{1}{M}+\frac{1}{\mu}\right)B^2 + E_g - E_b + \frac{\hbar^2 k^2}{2M}\left(1 - B_{ex2}\right) - B_{ex1} + \frac{\pi^2\hbar^2}{2\mu L^2}\right)}{k_B T}\right)^{\frac{\alpha}{1-\alpha}} + \left(1 - \frac{(1-\alpha)\left(\frac{3a_{ex}^2}{4}\left(\frac{1}{M}+\frac{1}{\mu}\right)B^2 + 4E_g - 4E_b + 4\frac{\hbar^2 k^2}{2M}\left(1 - 2B_{ex2}\right) - 8B_{ex1} + \frac{2\pi^2\hbar^2}{\mu L^2}\right)}{k_B T}\right)^{\frac{\alpha}{1-\alpha}}\right] \\ - \left[\left(1 - \frac{(1-\alpha)\left(\frac{3a_{ex}^2}{16}\left(\frac{1}{M}+\frac{1}{\mu}\right)B^2 + E_g - E_b + \frac{\hbar^2 k^2}{2M}\left(1 - B_{ex2}\right) - B_{ex1} + \frac{\pi^2\hbar^2}{2\mu L^2}\right)}{k_B T}\right)^{\frac{1}{1-\alpha}} + \left(1 - \frac{(1-\alpha)\left(\frac{3a_{ex}^2}{4}\left(\frac{1}{M}+\frac{1}{\mu}\right)B^2 + 4E_g - 4E_b + 4\frac{\hbar^2 k^2}{2M}\left(1 - 2B_{ex2}\right) - 8B_{ex1} + \frac{2\pi^2\hbar^2}{\mu L^2}\right)}{k_B T}\right)^{\frac{1}{1-\alpha}}\right] \\ + \left[\left(1 - \frac{(1-\alpha)\left(E_g - E_b + \frac{\hbar^2 k^2}{2M}\left(1 - B_{ex2}\right) - B_{ex1} + \frac{\pi^2\hbar^2}{2\mu L^2}\right)}{k_B T}\right)^{\frac{\alpha}{1-\alpha}} + \left(1 - \frac{(1-\alpha)\left(4E_g - 4E_b + 4\frac{\hbar^2 k^2}{2M}\left(1 - 2B_{ex2}\right) - 8B_{ex1} + \frac{2\pi^2\hbar^2}{\mu L^2}\right)}{k_B T}\right)^{\frac{\alpha}{1-\alpha}}\right] \\ + \left[\left(1 - \frac{(1-\alpha)\left(E_g - E_b + \frac{\hbar^2 k^2}{2M}\left(1 - B_{ex2}\right) - B_{ex1} + \frac{\pi^2\hbar^2}{2\mu L^2}\right)}{k_B T}\right)^{\frac{1}{1-\alpha}} + \left(1 - \frac{(1-\alpha)\left(4E_g - 4E_b + 4\frac{\hbar^2 k^2}{2M}\left(1 - 2B_{ex2}\right) - 8B_{ex1} + \frac{2\pi^2\hbar^2}{\mu L^2}\right)}{k_B T}\right)^{\frac{1}{1-\alpha}}\right]\end{array}\right] \quad (20)$$

3. Results and Discussions

This section presents numerical results and discussions of the theoretical formalisms and analytical results obtained in the previous section through calculations of some magnetic properties of exciton polaron in monolayers TMD quantum well such as magnetic susceptibility, magnetization and magnetocaloric effect. The values of the constants used here are

the same as in Refs. [20, 28]. For The numerical results, we consider all the TMD materials of 2H types comprising molybdenum diselenide ($MoSe_2$), molybdenum disulfide (MoS_2) tungsten diselenide (WSe_2) and tungsten disulfide (WS_2) [33].

We start this section with three dimensional representation of the magnetization versus magnetic field and quantum well length (Figure 1), then versus temperature and magnetic field (Figure 2), and versus temperature and quantum well length (Figure 3) for different TMD monolayers. These figures indicate that magnetization of the system is negative, characteristic of diamagnetism. The negative magnetization proved that the magnetic moment in the materials are on average, aligned antiparallel to the external field. We also observe a competition between thermal, magnetic and quantum confinement contributions on magnetization. In Figure 1, one can observe three regions: in the first region, the magnetization decreases until reaches a minimum, then increases in the second region and stabilizes in the third region. Thus, it can be suggested that the introduction of magnetic field contributes to the system to switch from its initial state, but also affects the system's electronic states. This alters the trajectory of the electrons and causes the direction of the orbital current to oppose that of the magnetic field, and generating a negative magnetization known as diamagnetism. Energy levels are shifted and Free energy become more sensitive to magnetic field, making the slope of magnetization becomes strongly negative. others reasons of free energy change are the change of energy level due to electron-hole confinement in the quantum well and the magnetic field effect on magnetic moment alignment. Contrary to other system where magnetization is monotonous, the non-monotonous magnetization here shows the competition between parameters dependent on magnetization. These parameters are temperature which led to population change, magnetic field and quantum confinement which favor one state over another. The minimum observed in the first region can be interpreted as the equilibrium of the competition between those parameters, also where the exciton-environment coupling is maximal, energy renormalization is strongest and represents the area where populations are changing most rapidly. In the second region, the magnetization increase, this increase in the magnetization is due to the fact that magnetic field opposition become less strong because the states most sensitive to the field are already occupied and the system has exhausted most of its reorganization capacity, making it enters a saturation regime. In the third region, we observed a saturation, this means that all the magnetic potential of the materials has been used up, every possible atomic spin is already aligned with field. The populations hardly change anymore, the system is practically static and further variations in the field no longer bring about significant changes. Magnetic sensitivity gradually disappears and the material becomes robust against further disturbances. This region corresponds to a highly polarized regime; and quasi-stabilized state. This type of response has several advantages, such as stability at high fields due to its predictable behavior and low sensitivity to fluctuations, which is very useful for quantum devices. Furthermore, it exhibits a high sensitivity region near the minimum, which is very important, making the material an excellent sensor because even small external variations produce a measurable response. Such a system also allows for adjustment because the minimum can be shifted by modifying the confinement, temperature, or magnetic field, thus fine-tuning the magnetic response. Moreover, In Figure 2 and Figure 3, in addition to the previous competition observed, it is clear that thermal contribution dominates and the magnetization ends as a decreasing function. However, $MoSe_2$ material requires higher field before reaching its maximum response, which gives it greater energy rigidity, allowing it to be more resistant to disturbances and making it more stable. This is due to its strong confinement and strong electron-phonon coupling. Its redistribution between states is therefore gradual and less sensitive than others material, even though its response remains more robust. Another observation is that WS_2 material exhibits a stronger opposition to the field because: its diamagnetic response is more intense, and its electronic states are more sensitive, making it the best magnetic detector because a small change in magnetic field produces a larger change in energy. This is justified by the strong coupling between the exciton and the field, creating a greater renormalization. WS_2 material is therefore the one that remains strongly magnetic for a long time. The results on magnetization can be used in magnetic refrigeration where materials with compensation points have huge entropy change, also in data storage where the magnetization can be switched from positive to negative value with just a laser pulse.

We depicted magnetic susceptibility versus magnetic field and quantum length (Figure 4), versus temperature and magnetic field (Figure 5), and versus temperature and quantum length (Figure 6). It is observed that contrary to pure diamagnetism system where the magnetic susceptibility is negative, our plots show a local Paramagnetism. On can also observe a competition between thermal, magnetic field and quantum confinement contributions on susceptibility. In Figure 4, we observe 4 regions. In the first region, the magnetic susceptibility reaches its absolute minimum, exhibiting negative values corresponding to a maximal diamagnetic state and showing high sensitivity resulting from the redistribution of populations. Then, the magnetic susceptibility increases in the second region passing through zero. This region is called a sign change in magnetic susceptibility characterize by the presence of two opposing magnetic mechanisms, and at that particular point where magnetic susceptibility is zero the two opposite mechanisms are cancel out. In the third region the magnetic susceptibility reaches it maximum, so after the contribution of the two opposing magnetic mechanisms, one wins and gives a peak before thermal disorder kills it. In this region, local Paramagnetism saturates. in the fourth region magnetic susceptibility decreases until reaches it second minimum at relaxation this means that thermal disorder is winning over magnetic ordering and fifth region it is stabilize. The stabilization means that the strong cooperative magnetism is gone. Only weak independent spins or constant electron contributions are left. The materials are now in a paramagnetic state, there are no more phase transitions. The introduction of magnetic field makes the system left it reference state and affect the electronics states. In these regions, diamag-

netic activity reaches its maximum efficiency, population redistribution becomes significant, and energy competition begins and gradually intensifies. This competition increases magnetic susceptibility until it cancels out, thus marking the point at which the competitions balance each other out. The negative diamagnetic contribution is compensated by the positive contribution of local Paramagnetism due to confinement effects and the magnetic field. This effective local Paramagnetism is amplified with the increase in the field, which affects the energy and population of the levels, but also with progressive confinement, which modifies the energy separation, thus making the susceptibility positive. The system becomes momently more sensitive to the field, but the peak decreases slightly once the local paramagnetic contribution also begins to saturate, corresponding to relaxation. The populations stabilize, but in a strong field, the system retains a residual positive sensitivity; in other words, the competitive mechanism survives even when the main diamagnetism is saturated. The dominant diamagnetic contribution is progressively challenged and then locally overtaken by a positive contribution linked to the reorganization of the system's states. Such a system is very useful for sensors because it provides magnetic control, as the system can be driven between a strong diamagnetic, quasi-neutral, and local paramagnetic response. Furthermore, it can provide fine-tuning because the peak can be shifted by the coupling as well as by the (L, B, T) parameters. Comparing the susceptibility of four materials with the same general topology is more informative than comparing magnetization, as it is a response parameter that directly indicates how the material reacts to magnetic perturbations. WS_2 Material exhibits a stronger local diamagnetic response because before competitive mechanisms come into play, WS_2 material opposes the field more strongly, making it more sensitive in the diamagnetic regime with excellent stability against weak magnetic perturbations. This could be explained by more effective confinement, greater orbital curvature, and its excitonic properties. Since the energy levels of $MoSe_2$ material is more widely spaced and its binding energy is higher, more magnetic energy is required to modify its internal structure, making it more rigid, unlike WS_2 material, which appears to be the most tunable with a more robust energy structure. However, at the peak, the redistribution of populations is greater in WS_2 material, which gives it very good magnetic sensitivity against less good stability.

In Figure 5, the same competition is observed but principally dominated by the magnetic contribution of susceptibility. This is explained by the fact that the magnetic field contributed to alignment of magnetic moment thus contribute to statistical redistribution, exciton-phonon renormalization and reorganization of energy levels. Unlike Figures 4 and 5, Figure 6 shows a completely negative or diamagnetic magnetic susceptibility with a competition between thermal and confinement contributions. Two regions are distinguished: the first, where susceptibility increases for molybdenum materials dominates by confinement, and the second, dominates by the temperature. The maximum corresponds to an equilibrium point of statistical redistribution and reorganization. Furthermore, for tungsten materials, there are three regions: the first is characterized by the dominance of thermal effects, the second by the confinement effect and the minimum corresponding to an equilibrium between energy levels and reorganization, and the last, a relaxation corresponding to a decrease in magnetic susceptibility.

Entropy change well known as magnetocaloric effect are shown in Figures 7-9. as function of quantum well length and magnetic field (Figure 7), of magnetic field and temperature (Figure 8), and quantum well length and temperature (Figure 9) for different 2D monolayers TMD of 2H types. These figures indicate that the entropy change decreases with both magnetic field and quantum well length whereas entropy change is increasing considerably with temperature. In Figure 7 and Figure 8, the entropy change is negative. We observe that upon the introduction of the magnetic field, the magnetic moments are aligned and the system is ordered, thus drastically reducing disorder, which explains the very rapid decrease observed. Indeed, before the field was applied, several states were accessible, but after its application, some states become energetically disadvantaged, and the number of actually occupied states decreases since the field partially lifts the degeneracies. Thus, the population concentrates in the lowest levels, and entropy decreases. At its minimum, the system reaches its maximum loss of disorder, and at that point, the field becomes most effective at reorganizing the populations. This is the region where the magnetocaloric effect is maximal. Since the field has already accomplished most of the ordering, the populations are almost fixed, and given that few states remain accessible, entropy cannot continue to decrease because it cannot more order the system which is already highly ordered. It is also noted that when the field is applied, disorder decreases under adiabatic conditions and the system temperature increases, leading to a regime known as the robust conventional magnetocaloric effect. This mechanism finds application in magnetic refrigerators, such as for heat conversion and thermal management using magnetic fields. WS_2 material, exhibiting a deeper minimum, appears to be the one whose field is most effective at reorganizing the system, making it the material with high magnetic response, high population variation, and significant energy competition among the four materials. It therefore has a greater magnetocaloric effect and can find applications in magnetic cooling, thermal control and thermomagnetic sensors. In Figure 9, The magnetic field thus reduces the number of accessible states, and the system becomes more ordered because it lifts degeneracies, selects certain energy states, and concentrates populations in a smaller number of states, thereby decreasing disorder. Another factor that makes the field extremely effective is that at low temperatures, thermal fluctuations are small, and populations are already concentrated in a few states. Therefore, temperature has virtually no effect on the order created by the field, and it acts almost independently, strongly ordering the material. As temperature increases, thermal excitations appear, the system begins to access more states, the order imposed by the field becomes less dominant, and the entropy change rises rapidly. A competition arises between magnetic order and thermal disorder. These ma-

terials offer several advantages: magnetic stability (the sign remains negative everywhere), energetic robustness (the field retains its influence even at high temperatures), gradual thermal control (the response can be finely tuned), predictable response, and a magnetocaloric effect exploitable over a wide temperature range due to its robustness and strong confinement. WS_2 material has the highest disappearance temperature at low entropy change, making it the excellent candidate of the four, as it retains its magnetocaloric properties for the longest period.

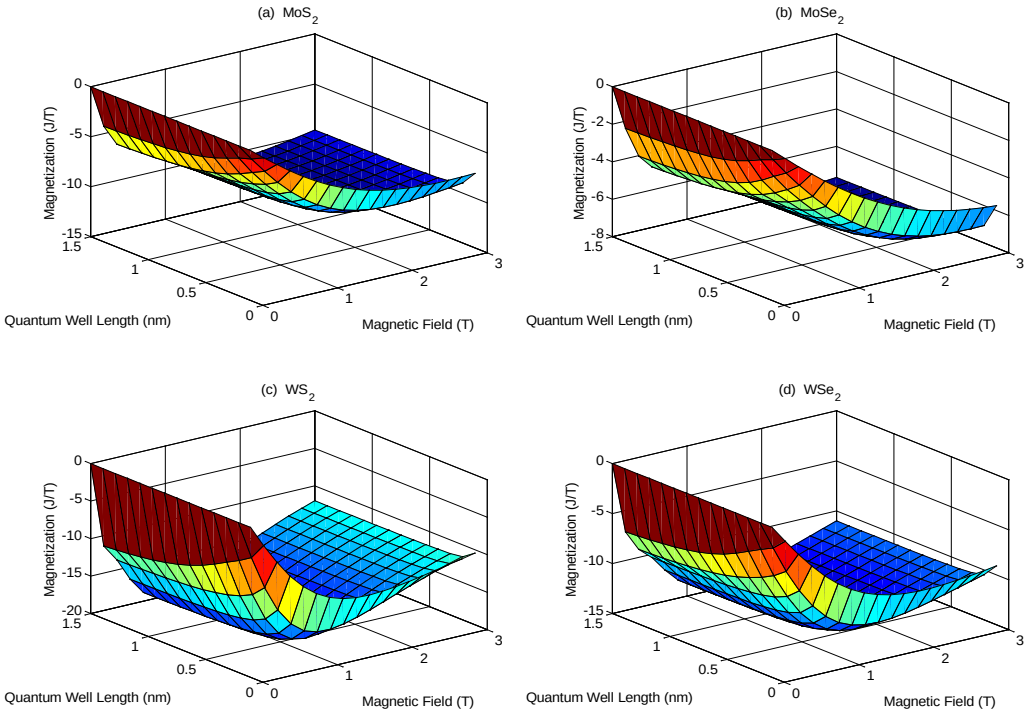

Figure 1. *Magnetization versus quantum well length and magnetic field for different TMDs monolayers: (a) MoS_2; (b) $MoSe_2$; (c) WS_2 and (d) WSe_2.*

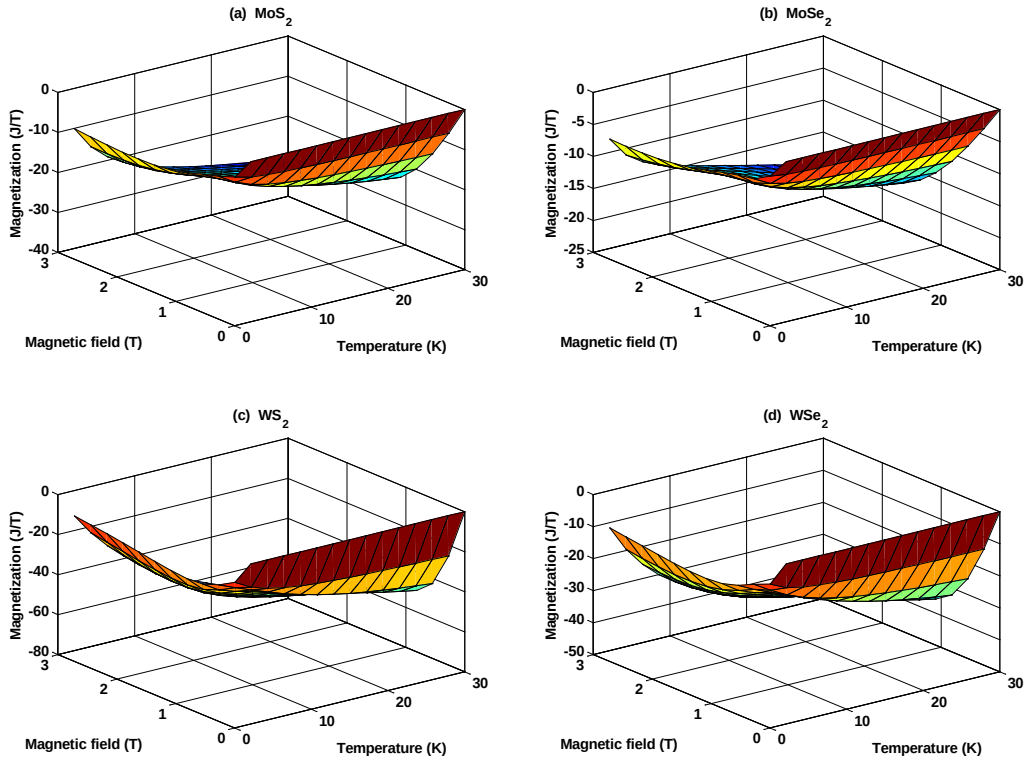

Figure 2. *Magnetization versus magnetic field and temperature for different TMDs monolayers: (a) MoS_2; (b) $MoSe_2$; (c) WS_2 and (d) WSe_2.*

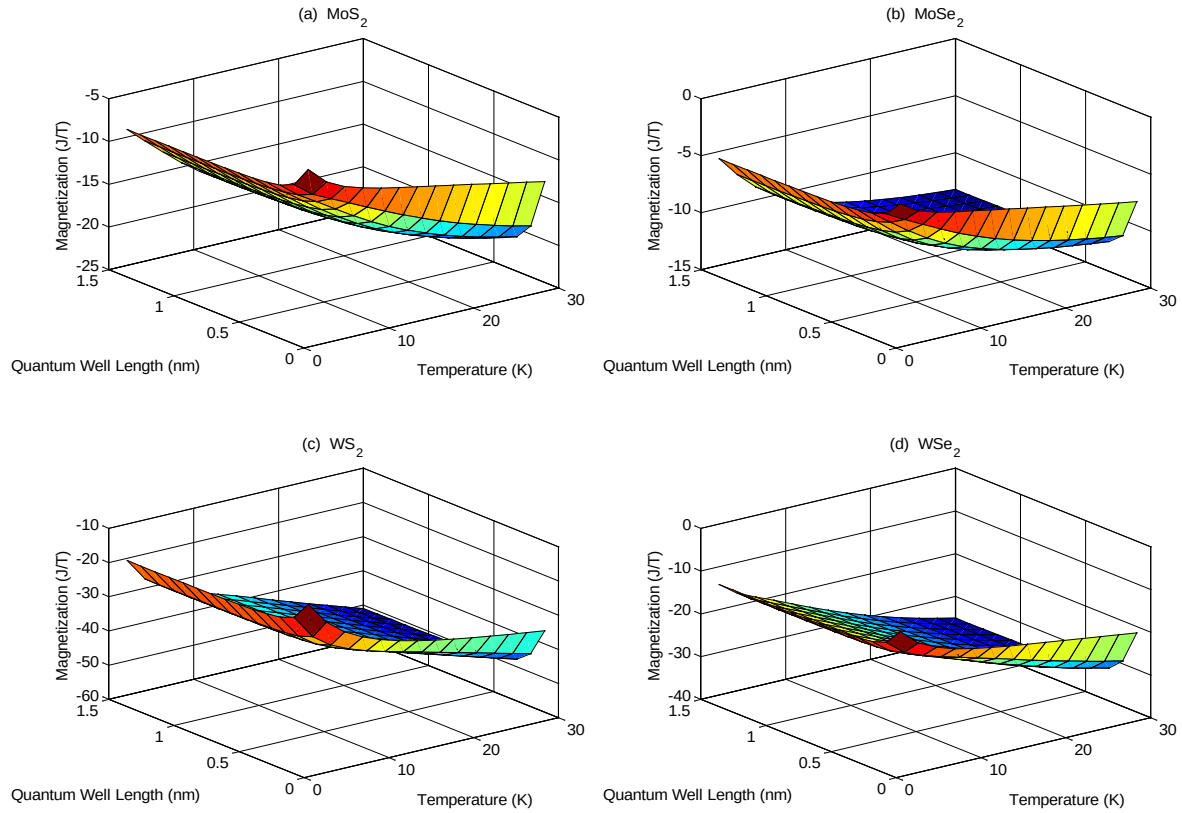

Figure 3. *Magnetization versus quantum well length and temperature for different TMDs monolayers: (a) MoS_2; (b) $MoSe_2$; (c) WS_2 and (d) WSe_2.*

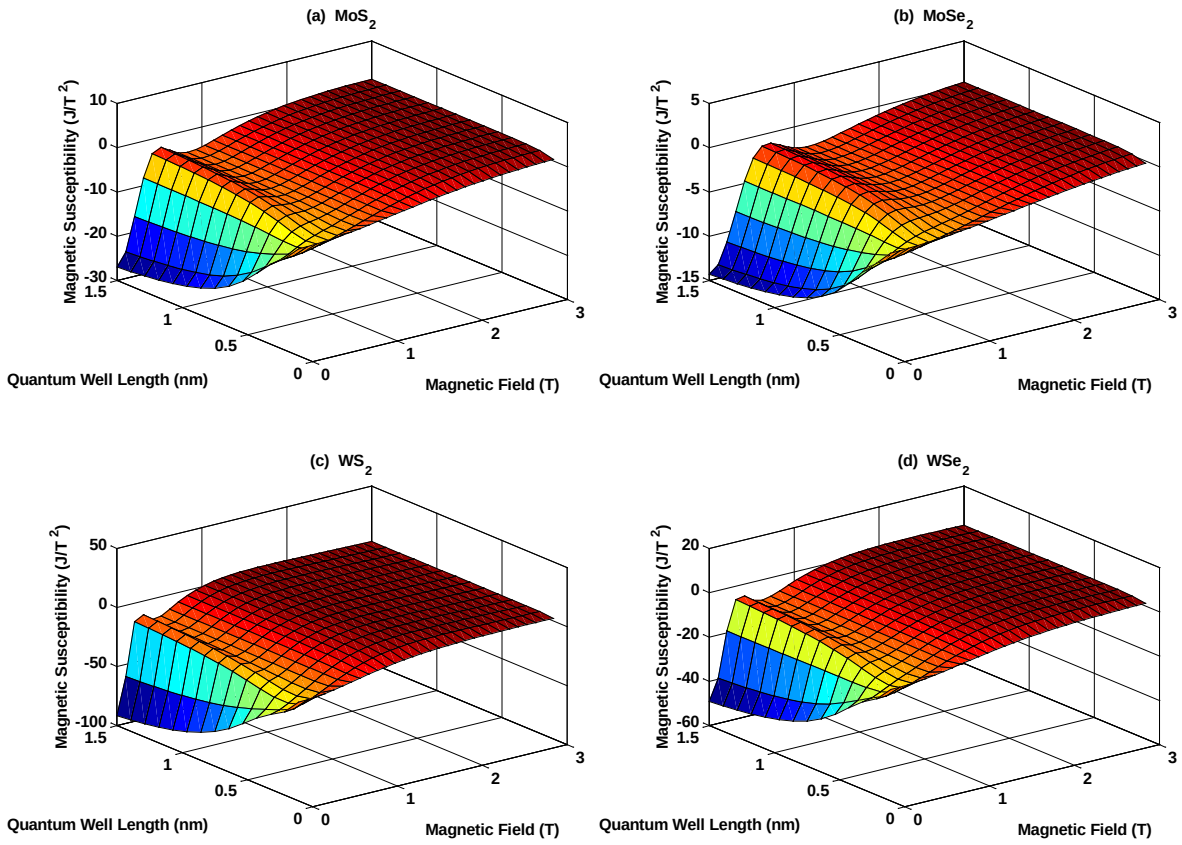

Figure 4. *Magnetic Susceptibility versus quantum well length and magnetic field for different TMDs monolayers: (a) MoS_2; (b) $MoSe_2$; (c) WS_2 and (d) WSe_2.*

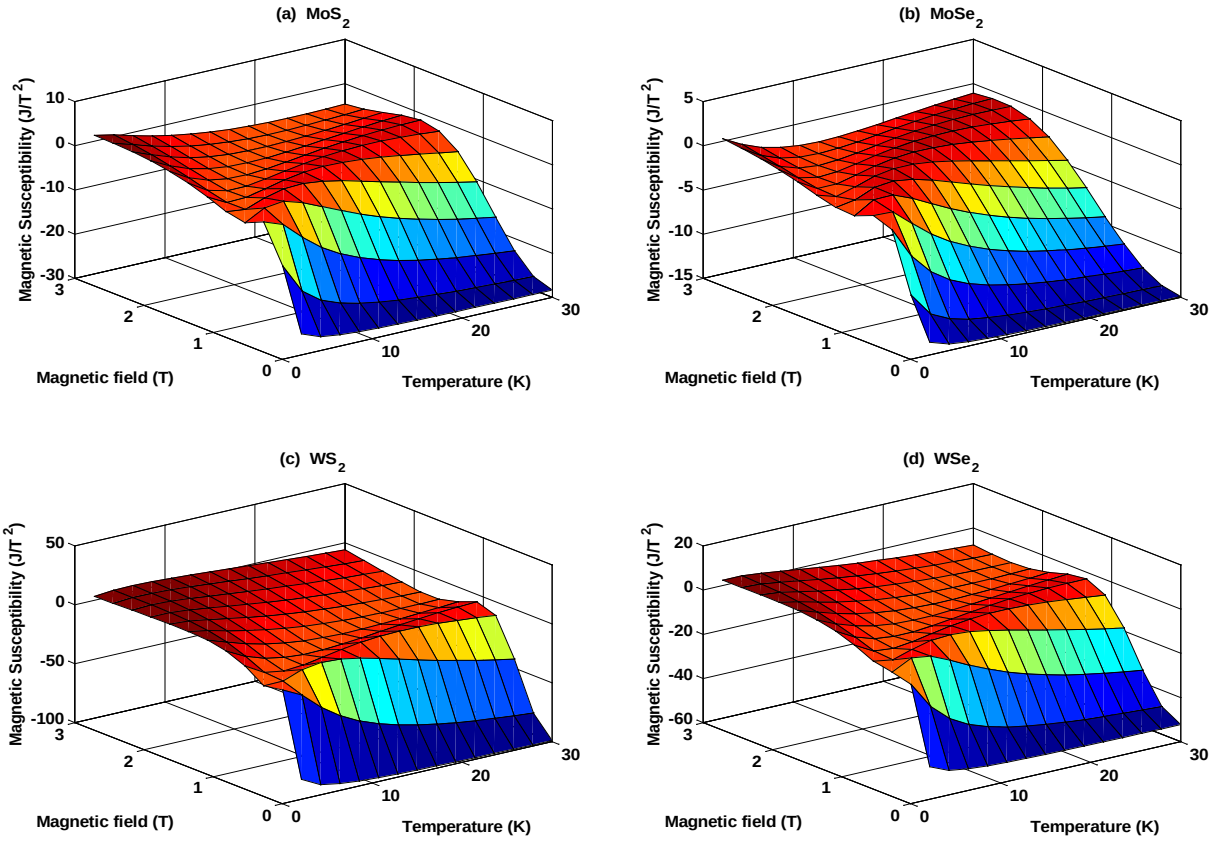

Figure 5. *Magnetic Susceptibility versus magnetic field and temperature for different TMDs monolayers: (a) MoS_2; (b) $MoSe_2$; (c) WS_2 and (d) WSe_2*

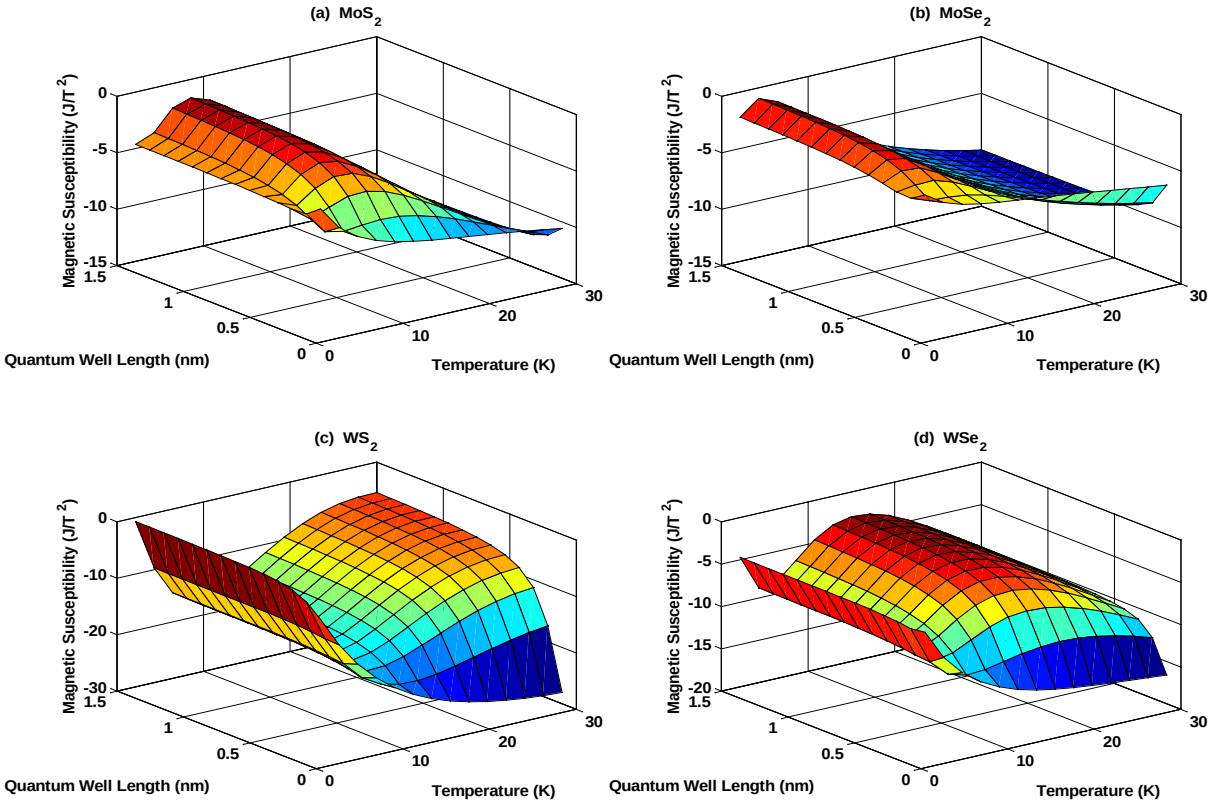

Figure 6. *Magnetic Susceptibility versus quantum well length and temperature for different TMDs monolayers: (a) MoS_2; (b) $MoSe_2$; (c) WS_2 and (d) WSe_2.*

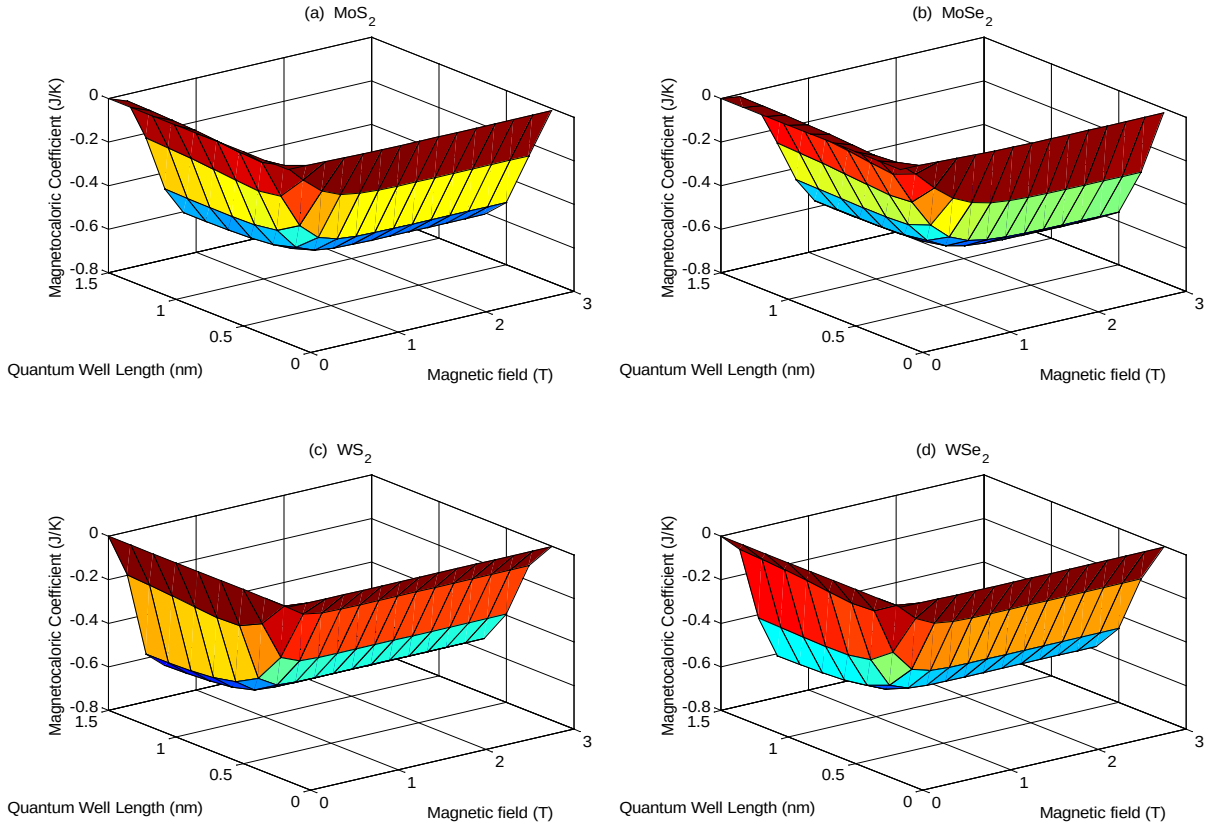

Figure 7. *Magnetocaloric Coefficient versus quantum well length and magnetic field for different TMDs monolayers: (a) MoS_2; (b) $MoSe_2$; (c) WS_2 and (d) WSe_2.*

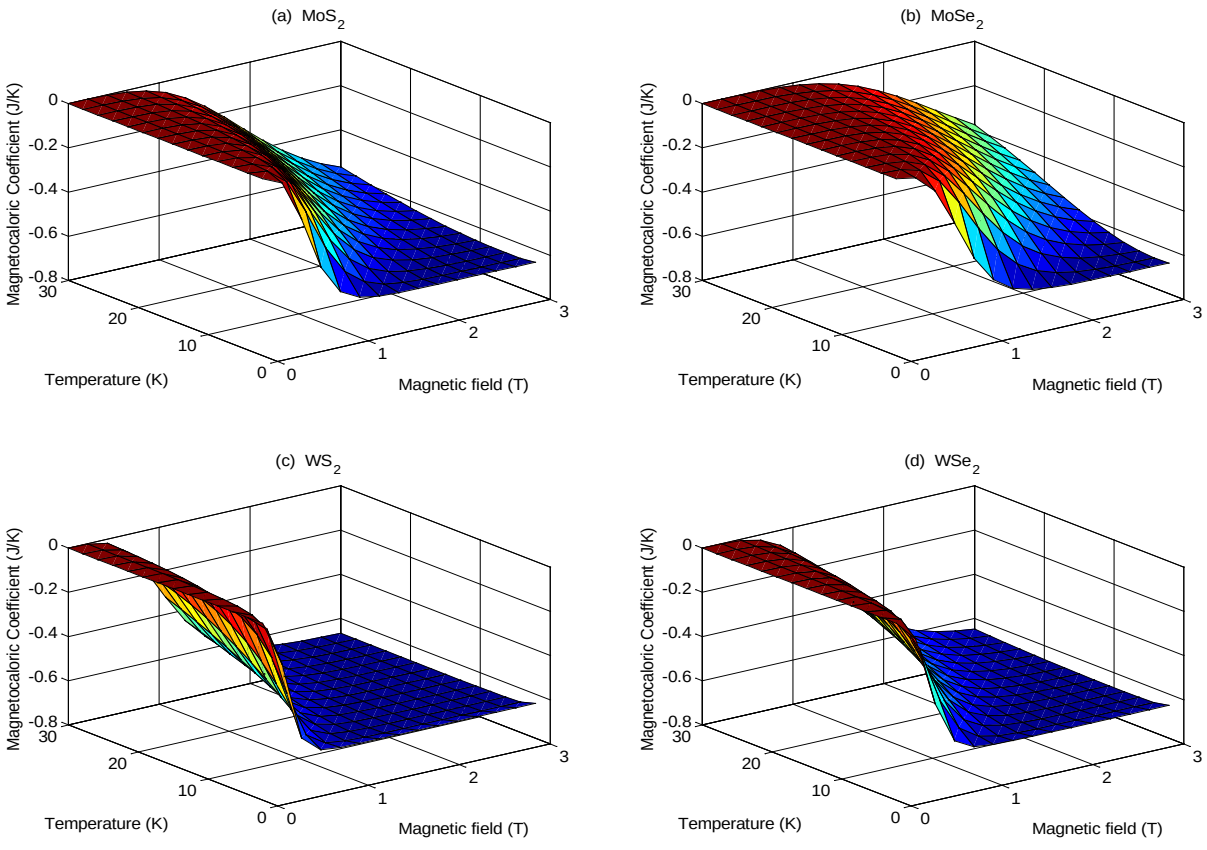

Figure 8. *Magnetocaloric Coefficient versus magnetic field and temperature for different TMDs monolayers: (a) MoS_2; (b) $MoSe_2$; (c) WS_2 and (d) WSe_2.*

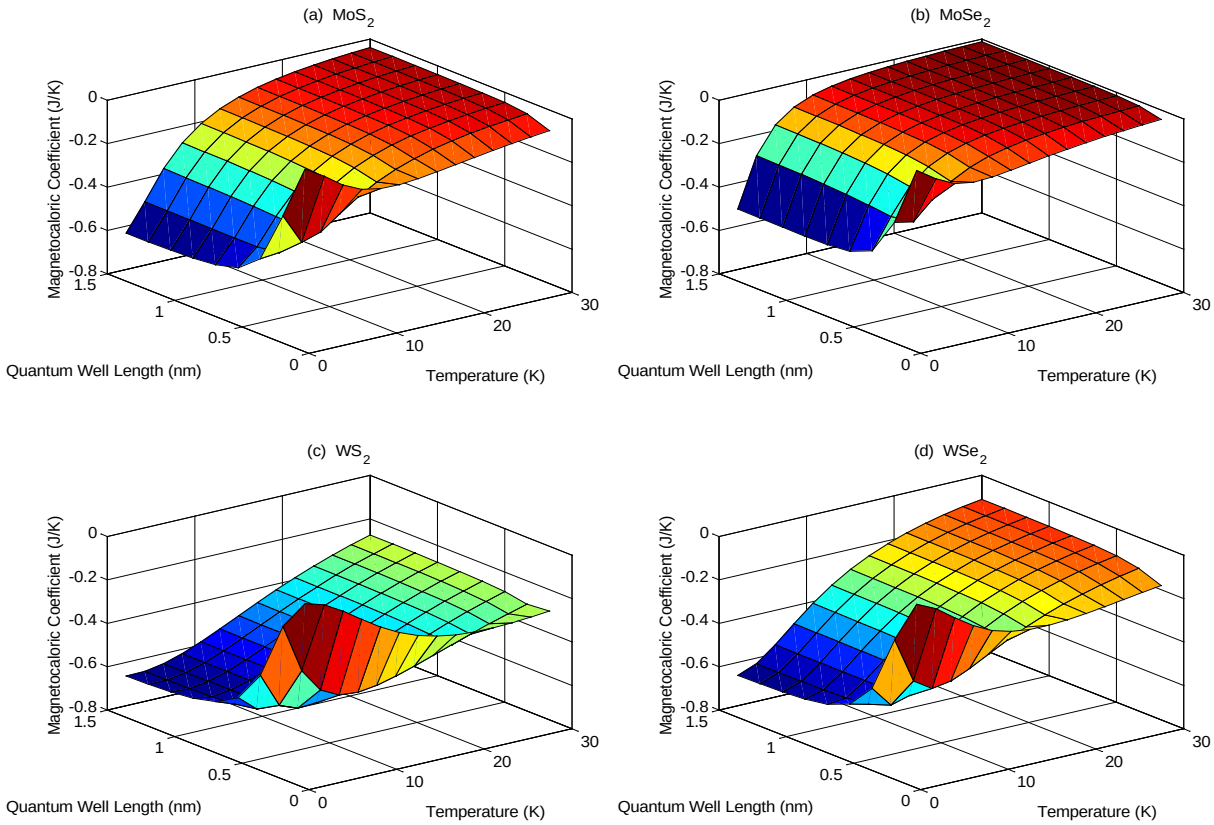

Figure 9. *Magnetocaloric Coefficient versus quantum well length and temperature for different TMDs monolayers: (a) MoS_2; (b) $MoSe_2$; (c) WS_2 and (d) WSe_2.*

4. Conclusion

In conclusion, the aims of this study was to investigate the of MCE and magnetic properties of exciton polaron in TMD quantum well. We use the grand canonical ensemble to evaluate the partition function and derived the magnetic susceptibility, the magnetization and the entropy exchange. Numerical results have shown that high magnetic field significantly affect the magnetic moment alignment and yield to statistical redistribution and reorganization of the level states. The exciton polaron magnetic properties are function of quantum length, magnetic field and temperature parameters which are always in competition. We also shown that dependent of the range of parameter, this competition can exhibit interesting behavior such as high conventional magnetocaloric effect, potential applications to sensitive thermomagnetic sensors, refrigerators. We also found that our system exhibits local paramagnetism and WS_2 material was more robust and sensitive whereas $MoSe_2$ material was more stable between the four materials studied. In addition to the temperature and the external magnetic field, the choice of quantum well length can also be used to control/modulate the variation magnetic properties and MCE of exciton polaron in 2D monolayer TMD.

Abbreviations

MCE	Magnetocaloric Effect
WS_2	Tungsten Disulfide
$MoSe_2$	Molybdenum Diselenide
MoS_2	Molybdenum Disulfide
WSe_2	Tungsten Diselenide
TMD	Transition Metal Dichalcogenide
CVD	Chemical Vapor Deposition
MBE	Molecular Beam Epitaxy
ALD	Atomic Layer Deposition
MFTs	Magnetic Flux-cored Transistors

Author Contributions

Edmond Ledoux Mbieda Posseu: Formal Analysis, Funding acquisition, Investigation, Methodology, Software, Writing – original draft, Writing – review & editing

Jean Valere Nguepnang: Conceptualization, Data curation, Methodology, Resources, Validation, Visualization, Writing – review & editing

Clautaire Mwebi Ekengoue: Methodology, Writing – review & editing

Arthur Kitio Teguimfouet: Investigation, Writing – review & editing

Gervi Mouketo Moussavou: Formal Analysis, Writing – review & editing

Christian Kenfack-Sadem: Project administration, Supervision, Validation, Writing – review &editing

Lukong Cornelius Fai: Project administration, Supervision, Validation

Conflicts of Interest

The authors declare no conflicts of interest.

References

[1] Wolfle, P. (2018). Quasiparticles in condensed matter systems. *Reports on Progress in Physics*, *81*(3), 032501. https://doi.org/10.1088/1361-6633/aa9bc4

[2] Weinberg, S. (1963). Quasiparticles and the Born series. *Physical Review*, *131*(1), 440. https://doi.org/10.1103/PhysRev.131.440

[3] Lieb, E. H., & Yamazaki, K. (1958). Ground-state energy and effective mass of the polaron. *Physical Review*, *111*(3), 728. https://doi.org/10.1103/PhysRev.111.728

[4] Landau, L. D. (1957). The theory of a Fermi liquid. *Soviet Physics Jetp-Ussr*, *3*(6), 920-925.

[5] Baym, G., & Pethick, C. (2008). Landau Fermi-liquid theory: concepts and applications.

[6] Mahan, G. D. (2013). *Many-particle physics*. Springer Science & Business Media.

[7] Altland, A., & Simons, B. D. (2010). *Condensed matter field theory*. Cambridge university press.

[8] Giuliani, G., & Vignale, G. (2008). *Quantum theory of the electron liquid*. Cambridge university press.

[9] Pustogow, A., Saito, Y., Lohle, A., Sanz Alonso, M., Kawamoto, A., Dobrosavljevic, V., & Fratini, S. (2021). Rise and fall of Landau's quasiparticles while approaching the Mott transition. *Nature communications*, *12*(1), 1571. https://doi.org/10.1038/s41467-021-21741-z

[10] Schober, H., & Rols, S. (2010). Excitations in condensed matter: vibrations and phonons. *French Neutron Scattering Society thematic school 10*, 3-136. https://doi.org/10.1051/sfn/2010001

[11] Ashcroft, N. W., & Mermin, N. D. (1976). Solid state physics.

[12] Liao, B., Qiu, B., Zhou, J., Huberman, S., Esfarjani, K., & Chen, G. (2015). Significant reduction of lattice thermal conductivity by the electron-phonon interaction in silicon with high carrier concentrations: A first-principles study. *Physical review letters*, *114*(11), 115901. https://doi.org/10.1103/PhysRevLett.114.115901

[13] Frohlich, H. (1954). Electrons in lattice fields. *Advances in Physics*, *3*(11), 325-361. https://doi.org/10.1080/00018735400101213

[14] Wannier, G. H. (1937). The structure of electronic excitation levels in insulating crystals. *Physical Review*, *52*(3), 191. https://doi.org/10.1103/PhysRev.52.191

[15] Bartsch, G., Gerbracht, M., Yakovlev, D. R., Blokland, J. H., Christianen, P. C. M., Zhukov, E. A, & Bayer, M. (2011). Positively versus negatively charged excitons: A high magnetic field study of CdTe/Cd 1-x Mg x Te quantum wells. *Physical Review B—Condensed Matter and Materials Physics*, *83*(23), 235317. https://doi.org/10.1103/PhysRevB.83.235317

[16] Chang, Y. W., & Reichman, D. R. (2019). Many-body theory of optical absorption in doped two-dimensional semiconductors. *Physical Review B*, *99*(12), 125421. https://doi.org/10.1103/PhysRevB.99.125421

[17] Berkelbach, T. C., Hybertsen, M. S., & Reichman, D. R. (2013). Theory of neutral and charged excitons in monolayer transition metal dichalcogenides. *Physical Review B—Condensed Matter and Materials Physics*, *88*(4), 045318. https://doi.org/10.1103/PhysRevB.99.125421

[18] Katsch, F., & Knorr, A. (2022). Excitonic theory of doping-dependent optical response in atomically thin semiconductors. *Physical Review B*, *105*(4), 045301. https://doi.org/10.1103/PhysRevB.105.045301

[19] Chang, Y. C., Shiau, S. Y., & Combescot, M. (2018). Crossover from trion-hole complex to exciton-polaron in n-doped two-dimensional semiconductor quantum wells. *Physical Review B*, *98*(23), 235203. https://doi.org/10.1103/PhysRevB.98.235203

[20] Wang, G., Chernikov, A., Glazov, M. M., Heinz, T. F., Marie, X., Amand, T., & Urbaszek, B. (2018). Colloquium: Excitons in atomically thin transition metal dichalcogenides. *Reviews of Modern Physics*, *90*(2), 021001. https://doi.org/10.1103/RevModPhys.90.021001

[21] Chen, H. Y., Sangalli, D., & Bernardi, M. (2020). Exciton-phonon interaction and relaxation times from first principles. https://doi.org/10.48550/arXiv.2002.08913

[22] Christiansen, D., Selig, M., Berghauser, G., Schmidt, R., Niehues, I., Schneider, R., & Knorr, A. (2017). Phonon sidebands in monolayer transition metal dichalcogenides. *Phys. Rev. Lett*, *119*(18), 187402. https://doi.org/10.1103/PhysRevLett.119.187402

[23] Paleari, F., & Marini, A. (2022). Exciton-phonon interaction calls for a revision of the" exciton" concept. *arXiv preprint*. https://doi.org/10.48550/arXiv.2205.02783

[24] Yu, H., Du, L., Tang, J., Zhang, Q., Zhang, G., Liao, M. & Taniguchi, T. (2018). Strongly enhanced exciton-phonon coupling in two-dimensional WS e 2. *Physical Review B*, *97*. https://doi.org/10.1103/physrevb.97.235145

[25] Carvalho, B. R., Malard, L. M., Alves, J. M., Fantini, C., & Pimenta, M. A. (2015). Symmetry-dependent exciton-phonon coupling in 2D and bulk MoS 2 observed by resonance Raman scattering. *Physical review letters*, *114*(13), 136403. https://doi.org/10.1103/PhysRevLett.114.136403

[26] Thilagam, A. (2015). Excitonic polarons in low-dimensional transition metal dichalcogenides. *Physica B: Condensed Matter*, *464*, 44-50. https://doi.org/10.1016/j.physb.2015.02.015

[27] Henriques, J. C. G., & Peres, N. M. R. (2021). Perturbative approach to the polaron shift of excitons in transition metal dichalcogenides. *Physical Review B*, *103*(16), L161402. https://doi.org/10.1103/PhysRevB.103.L161402

[28] Novoselov, K. S., Jiang, D., Schedin, F., Booth, T. J., Khotkevich, V. V., Morozov, S. V., & Geim, A. K. (2005). Two-dimensional atomic crystals. *Proceedings of the National Academy of Sciences*, *102*(30), 10451-10453. https://doi.org/10.1073/pnas.0502848102

[29] Mak, K. F., Lee, C., Hone, J., Shan, J., & Heinz, T. F. (2010). Atomically thin MoS 2: a new direct-gap semiconductor. *Physical review letters*, *105*(13), 136805. https://doi.org/10.1103/PhysRevLett.105.136805

[30] Splendiani, A., Sun, L., Zhang, Y., Li, T., Kim, J., Chim, C. Y.,.. & Wang, F. (2010). Emerging photoluminescence in monolayer MoS_2. *Nano letters*, *10*(4), 1271-1275. https://doi.org/10.1021/nl903868w

[31] Choi, W., Choudhary, N., Han, G. H., Park, J., Akinwande, D., & Lee, Y. H. (2017). Recent development of two-dimensional transition metal dichalcogenides and their applications. *Materials Today*, *20*(3), 116-130. https://doi.org/10.1016/j.mattod.2016.10.002

[32] Mueller, T., & Malic, E. (2018). Exciton physics and device application of two-dimensional transition metal dichalcogenide semiconductors. *npj 2D Materials and Applications*, *2*(1), 29. https://doi.org/10.1038/s41699-018-0074-2

[33] Yilmaz, E., & Yavuz, E. (2024). Use of transition metal dichalcogenides (TMDs) in analytical sample preparation applications. *Talanta*, *266*, 125086. https://doi.org/10.1016/j.talanta.2023.125086

[34] Hu, X., Yan, L., Ding, L., Zheng, N., Li, D., Ji, T.,.. & Hu, J. (2024). Structural regulation and application of transition metal dichalcogenide monolayers: Progress and challenges. *Coordination Chemistry Reviews*, *499*, 215504. https://doi.org/10.1016/j.ccr.2023.215504

[35] Wang, Q. H., Kalantar-Zadeh, K., Kis, A., Coleman, J. N., & Strano, M. S. (2012). Electronics and optoelectronics of two-dimensional transition metal dichalcogenides. *Nature nanotechnology*, *7*(11), 699-712. https://doi.org/10.1038/nnano.2012.193

[36] Huang, X., Liu, C., & Zhou, P. (2022). 2D semiconductors for specific electronic applications: from device to system. *npj 2D Materials and Applications*, *6*(1), 51. https://doi.org/10.1038/s41699-022-00327-3

[37] Peng, Z., Chen, X., Fan, Y., Srolovitz, D. J., & Lei, D. (2020). Strain engineering of 2D semiconductors and graphene: from strain fields to band-structure tuning and photonic applications. *Light: Science & Applications*, *9*(1), 190. https://doi.org/10.1038/s41377-020-00421-5

[38] Srivastava, A., Sidler, M., Allain, A. V., Lembke, D. S., Kis, A., & Imamoglu, A. (2015). Valley Zeeman effect in elementary optical excitations of monolayer WSe 2. *Nature Physics*, *11*(2), 141-147. https://doi.org/10.1038/nphys3203

[39] Chernikov, A., Berkelbach, T. C., Hill, H. M., Rigosi, A., Li, Y., Aslan, B., & Heinz, T. F. (2014). Exciton binding energy and nonhydrogenic Rydberg series in monolayer WS 2. *Physical review letters*, *113*(7), 076802. https://doi.org/10.1103/PhysRevLett.113.076802

[40] Thygesen, K. S. (2017). Calculating excitons, plasmons, and quasiparticles in 2D materials and van der Waals heterostructures. *2D Materials*, *4*(2), 022004. https://doi.org/10.1088/2053-1583/aa6432

[41] Xiao, D., Liu, G. B., Feng, W., Xu, X., & Yao, W. (2012). Coupled spin and valley physics in monolayers of MoS 2 and other group-VI dichalcogenides. *Physical review letters*, *108*(19), 196802. https://doi.org/10.1103/PhysRevLett.108.196802

[42] Chen, Y. J., Cain, J. D., Stanev, T. K., Dravid, V. P., & Stern, N. P. (2017). Valley-polarized exciton-polaritons in a monolayer semiconductor. *Nature Photonics*, *11*(7), 431-435. https://doi.org/10.1038/nphoton.2017.86

[43] Reis, M. S. (2015) Magnetocaloric cycle with six stages: possible applications of graphene at low temperature *Appl. Phys. Lett*. 107 (10), 102401. https://doi.org/10.1063/1.4930577

[44] Tarasenko R., et al. (2018). Experimental study of magnetocaloric effect in two-level quantum system $KTm(MoO_4)_2$ *Phys. B Condens. Matter 536* 450-453 https://doi.org/10.1016/j.physb.2017.09.083

[45] Alisultanov Z. Z. (2014). Oscillating magnetocaloric effect in size quantum diamagnetic film *J. Appl. Phys. 115* (11) 113913 https://doi.org/10.1063/1.4869237

[46] Y Y Gong, D H Wang, Q Q Cao, E K Liu, J Liu and Y W Du Adv. Mater. 27 801 (2015).

[47] Alisultanov, Z. Z., Paixao, L. S. and Reis, M. S. (2014). Oscillating magnetocaloric effect on a multilayer graphene. *Appl. Phys. Lett. 105* (23), 232406 https://doi.org/10.1063/1.4903833

[48] Sedehi, H. R. and Khordad, R. (2021). Magnetocaloric effect, magnetic susceptibility and specific heat of tuned quantum dot/ring systems. *Phys. E Low-Dimens. Syst. Nanostruct. 134*, 114886 https://doi.org/10.1016/j.physe.2021.114886

[49] Donfack, B., Nguepnang, J. V., Nguemassong, S. C. N., Temdie, L., Manfouo, F., Tchida, V. D., Magouwo, L. D., Kamdem, E. F., Kenfack, C. S., and Fotue, A. J. (2024). Magnetocaloric effect (MCE) of a quantum pseudodot. *Indian Journal of Physics. 98* (3); 997-1005. https://doi.org/10.1007/s12648-023-02871-0

[50] Nguepnang, J. V., Donfack, B., Ekengoue, C. M., Mbieda-Posseu, E. L., Tchamdjeu, F. N., Nganfo, W., & Kenfack-Sadem, C. (2025). Magnetocaloric Effect and Thermodynamic Properties of Trapped Polarons in 2D Monolayers Transition Metal Dichalcogenides. *Journal of Low Temperature Physics*, *220*(3), 173-191. https://doi.org/10.1007/s10909-025-03298-z

[51] Kenfack-Sadem, C., Nguepnang, J. V., Kenfack-Jiotsa, A., Mbognou, F. F., Diffo, T. V., & Hounkonnou, M. N. (2021). Magnetic effect on dynamic and decoherence of exciton polaron in transition metal dichalcogenides. *Physica Scripta*, *96*(12), 125824. https://doi.org/10.1088/1402-4896/ac2680

[52] Teguimfouet, A. K., Kenfack-Sadem, C., Kenfack-Jiotsa, A., Mbognou, F. F., El-Yadri, M., Perez, L. M. & Feddi, E. (2022). Magnetic barrier and temperature effects on optical and dynamic properties of exciton-polaron in monolayers transition metal dichalcogenides. *Physica E: Low-dimensional Systems and Nanostructures*, *144*, 115448. https://doi.org/10.1016/j.physe.2022.115448